ACERP: Vol. 5, No. 4, (Fall 2019) 17-23

Advanced Ceramics Progress

Research Article

Journal Homepage: www.acerp.ir

Mechanical Properties of Electrophoretically Deposited 45S5 Bioglass-Graphene Oxide Composite Coatings

P. Eshghinejad [a], H. Farnoush [a] *

[a] *Department of Metallurgy and Materials Engineering, Faculty of Engineering, University of Kashan, Kashan, Iran*

PAPER INFO

Paper history:

Received 22 October 2019
Accepted in revised form 25 December 2019

Keywords:

Bioglass
Graphene Oxide
Bonding
Scratch
Fracture Toughness

ABSTRACT

Bioglass-graphene oxide composites can be served as an appropriate alternative for bone implant applications due to its specific mechanical properties. In this study, the 45S5 bioactive glass (BG) - graphene oxide (GO) composite containing 2wt% GO was deposited on the Ti-6Al-4V alloy substrate via the electrophoretic deposition process (EDP). The synthesized GO was incorporated into BG coating to improve the mechanical properties. The phase, structural agents, microstructure, and composition were investigated by X-ray diffraction (XRD), Fourier transform infrared spectroscopy (FTIR), and scanning electron microscopy (SEM) equipped with energy dispersive spectroscopy (EDS), respectively. The micro scratch test with a progressive load was applied to study the adhesion and fracture toughness of coatings based on a linear elastic fracture mechanics model. micro scratch results showed the highest critical distances of crack initiation and delamination, critical contact pressures (P_{c1} and P_{c2}= 4.80 and 5.37GPa, respectively), and fracture toughness (K_{IC}= 0.885 MPa.$m^{1/2}$) for BG-GO composite coatings.

1. INTRODUCTION

The 45S5 bioglass (BG) can be utilized as an implant in tissue engineering with an improved biocompatibility over other implants [1]. However, the poor mechanical properties of bulk BG restricted it for utilization in biomedical applications [2]. Besides, Ti-6Al-4V has appealed a significant attention for biomedical applications due to its high specific strength, lightweight, prominent resistance to corrosion and chemical reactions, low elastic modulus and proper biocompatibility [3,4]. However, the deposition of bioactive glass coatings on Ti alloys has been found to provide a further enhancement in osteoinductive properties [3]. Electrophoretic deposition (EPD) is a low-cost method, which is effectively carried out for the formation of uniform bioglass coatings on the substrates with different shapes [5]. The EPD process constitutes the movement of charged particles in a stabilized suspension affected by an electric field, followed by deposition onto a substrate with the opposite charge [6]. One of the compounds used to improve the mechanical properties of bioglass is graphene oxide that has recently been widely used as the reinforcement in nanocomposites with applications in biomedical implants [7]. Also, graphene oxide has high conductivity, high specific surface, and favorable mechanical properties, better than carbon nanotubes [8]. Some studies showed that graphene oxide also can improve the toughness of brittle materials, which is a rich level for surface chemistry because of its high theoretical specific surface [8].

To the best of our knowledge, there is no work reporting the effect of graphene oxide on mechanical properties of electrophoretically deposited BG-GO composite coatings. In the present study, the bonding strength and fracture toughness of coated composites were evaluated by micro scratch analysis. In this regard, a linear elastic fracture mechanics model was applied to investigate the effect of GO content on fracture toughness of BG-GO composite coatings.

2. EXPERIMENTAL PROCEDURES

2.1. Synthesis of bioglass and graphene oxide

The 45S5 bioglass powders were synthesized by a sol-gel method [1]. First, the hydrolyzation process occurred by the dropwise addition of 11.6ml tetraethyl orthosilicate (TEOS) (Merck, Germany), and 1ml triethyl phosphate (TEP) (Merck, Germany) into 26ml

* Corresponding Author Email: farnoush@kashanu.ac.ir (H. Farnoush)

of 2M nitric acid at room temperature. Then, 4.66g sodium nitrate $NaNO_3$, $Ca(NO_3)_2 \cdot 4\ H_2O$ (Merck, Germany) was slowly added to the sol in 1h. The prepared sol was then kept for 10 days at room temperature in a capped container for the occurrence of hydrolysis and polymerization reactions. It was kept at 80ºC for 24h to vaporize all its water content after obtaining the gel. The dried gel was then calcined at 700ºC for 2h to obtain white bioglass powders.

The modified Hummers method was used for the synthesis of GO powder from the commercial graphite powder (Sigma-Aldrich, <20µm, >99.99wt% purity) [9]. The volume of 23ml concentrated sulfuric acid was added to a mixture of 1g graphite and 0.50g sodium nitrate. The mixture was kept for 10min at 0ºC in a bath-ice container under vigorous stirring. Then, 3g of potassium permanganate was gradually added to the mixture and the temperature was maintained at 5ºC for 2h. The solution was slowly heated to 35ºC and kept for 1h under stirring. The volume of 180ml deionized water and 10ml hydrogen peroxide was added to the mixture. The temperature increased to 98ºC and the resultant mixture was stirred for 1h due to the exothermic reaction of hydration. Finally, the brown/yellowish color product was centrifuged and washed repeatedly at a spinning speed of 9000rpm and a time of 30min for 5 times until the pH was neutral. The phase structure of synthesized GO and coatings was identified by X-ray diffractometer (XRD, X-pert P'analytical) using Cu-Kα radiation (λ = 0.154nm) at 40kV and 30mA with a scan range between 10-80º at a step of 0.02º and a scanning speed of $2^{\circ}.min^{-1}$. The structural agents were characterized by Fourier transform infrared (FT-IR, Magna-IR 550) spectroscopy in the wavenumber range of 4000–400cm^{-1}.

2.2. EPD of BG-GO composites

The synthesized BG and GO powders were used as coating materials. Suspensions of $20g.L^{-1}$ BG-GO composites with 0 and 2wt% GO (designated by BG and BG-2GO, respectively) were prepared by dispersing the desired amount of powders and $9m.L^{-1}$ triethanolamine (TEA), as the dispersant, in isopropanol alcohol (99.5, Merck, Germany).

Biomedical grade Ti-6Al-4V coupons with dimensions of $10\times20\times3mm^3$ were used as cathode substrates against 316L stainless steel anode. The electrodes were separated parallel to each other with a distance of 10mm in a 50mL glass beaker. Suspensions were sonicated for 20 min to obtain stable dispersions using an ultrasonic vibrator before each deposition. The EPD process was carried out at a constant DC voltage of 80V for 300s. Afterwards, the coated samples were dried in air condition at room temperature for 24h. To improve coating adhesion, the coated samples were sintered in a vacuum tube furnace at 800ºC for 1h with a heating rate of $5^{\circ}C.min^{-1}$ under argon backfilling. The microstructure and elemental composition of coatings were studied by field emission scanning electron microscopy (FE-SEM, Mira3-XMU) equipped with energy-dispersive X-ray spectroscopy (EDS, Mira3-XMU).

2.3. Micro scratch test

The mechanical behavior of coatings was studied by using a micro scratch tester (CSM Instruments). Scratching was conducted under a progressive load with a 200µm radius diamond indenter (Rockwell T-256). The normal load applied to the indenter was increased linearly from 0.05 to 10N at a scratch speed of $1.01mm.min^{-1}$ along a 2mm distance. The variation of normal force (F_n), tangential force (F_t), friction coefficient, penetration depth (P_d), and acoustic emission (AE) in terms of scratch distance was recorded by the Scratch V3.76 software. The critical normal loads refer to initial cracking, Lc1, and total delamination, L_{c2}, of the coating were measured as the adhesion of the coating. Five scratches were made on each of the substrates. The mean values of L_{c1} and L_{c2} were obtained by using acoustic emission profile vs. scratch distance. The scratch paths were analyzed by using a scanning electron microscope (SEM, Mira3-XMU). Moreover, a novel micro scratch technique was applied to assess the fracture toughness from the recorded forces and depth of penetration [10].

3. RESULTS AND DISCUSSION

3.1. Characterization of synthesized GO and BG-GO coating

Figure 1a shows the FE-SEM micrograph of synthesized GO powders. As seen, the thin and homogeneous sheets of graphene oxide have a layer thickness of 37nm. The twisted and crimped surfaces are recognizable from the edges of each sheet. Based on the XRD pattern in Figure 1b, the highest peak is around $2\theta=11.2^{\circ}$, indicating the major reflection of (001) plane for the GO phase [11].

Figure 1c shows the FT-IR spectrum of graphene oxide. The highest peak in $13340cm^{-1}$ relates to the expansion and bending vibration of OH^- groups of graphene-adsorbed water molecules, which results in high water-saturation of the synthesized sample. Absorption peaks in $11736cm^{-1}$ correspond to a strong bond of C = O carbonyl groups. A peak of $11630cm^{-1}$ can be related to the vibrational expansion of C=C groups of carboxylic acid. Finally, the absorption peaks in $11385cm^{-1}$ and $11110cm^{-1}$ correspond to the vibrational expansion of C-OH groups of alcohol and C-O carboxylic acid. The presence of oxygen in these groups indicates that the graphite is properly oxidized. Polar groups, in particular, hydroxyl groups, lead to the formation of hydrogen bonds between graphite and water molecules, which leads to the hydrophobicity of graphene oxide [11]. The characterization results obtained in comparison with the results of similar tasks indicate the successful synthesis of GO [12,13]

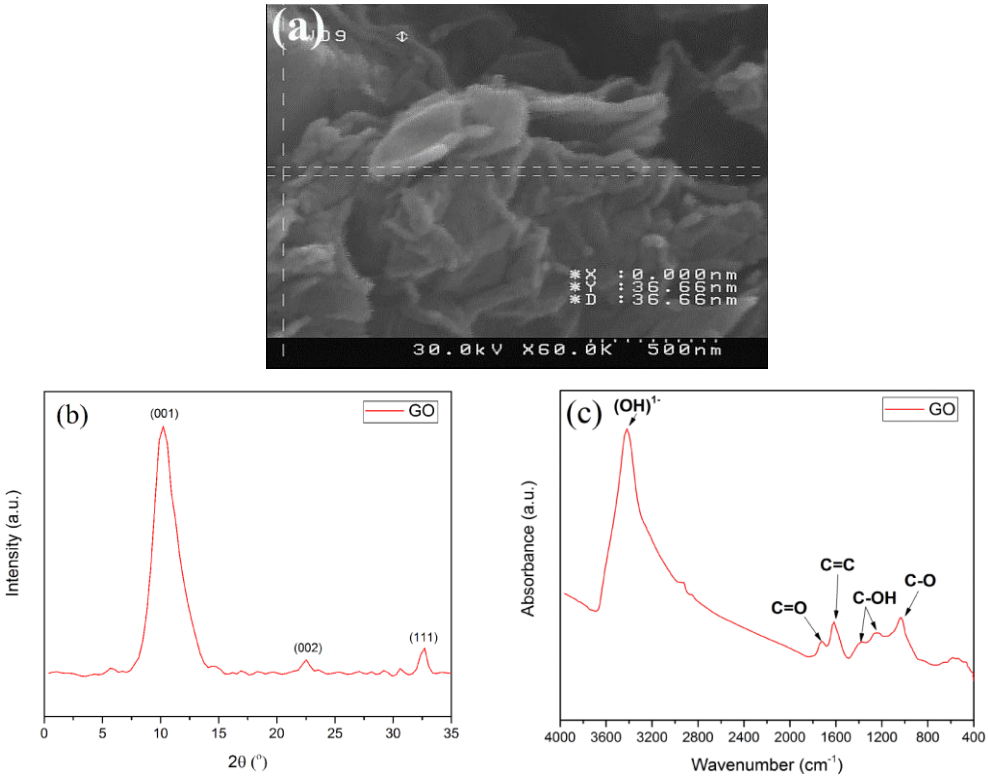

Figure 1. (a) FE-SEM micrograph, (b) XRD pattern and (c) FTIR spectrum of the synthesized GO

Figure 2 shows the SEM micrographs and EDS analysis from cross-sectional views of BG and BG-2GO coatings, which indicates a thickness of about 50µm for both films. The dense, crack-free, and uniform interface formed after sintering of both samples. Obviously, the incorporation of GO into the BG coating did not affect the thickness. According to EDS analysis, the weight percentage of GO in the combination of BG-2GO composites was 32.78%.

X-ray diffraction patterns of BG and BG-2GO coatings are illustrated in Figure 3. The characteristic peaks at 24, 27, 33, and 34° with miller indicators of (211), (122), (220), and (404) indicate the presence of the combeite phase ($Na_2Ca_2Si_3O_9$). Among several crystalline sodium calcium silicate phases inside the amorphous structure of the bioactive glass, combeite is the most interesting one as it is known to influence the bioactivity and solubility in SBF solution [14]. Moreover, the specified peaks in 32 and 49° with miller indices (143) and (312), confirms the presence of $Na_2CaSi_2O_6$ phase. Also, the major reflection of (001) plane for the GO phase was observed around $2\theta=11^{\circ}$ for the BG-2GO sample.

3.2. Mechanical properties

The bonding strength of coatings was obtained from micro scratch tests by the calculation of critical contact pressures according to Hertz's theory [10]:

$$p_c = \frac{2}{3}\left(\frac{6L_cE^{*2}}{\pi^3R^2}\right)^{\frac{1}{3}} \quad (1)$$

where L_c is the critical normal force, R is the radius of the indenter, and E* is the reduced Young modulus.

The reduced Young modulus was calculated using the following relation [15]:

$$\frac{1}{E^*} = \frac{\left(1-\upsilon_i^2\right)}{E_i} + \frac{\left(1-\upsilon_s^2\right)}{E_s} \quad (2)$$

Where ν_s and ν_i are the Poisson ratios of the sample and indenter, respectively, and E_s (= 113.8GPa) and E_i (=1050GPa) are the Young's moduli of the substrate and indenter, respectively. It is possible to recognize the Lc values by studying the acoustic emission variations (AE%) against scratch distance (or F_n). Figure 4 illustrates the initiation of the AE variation under L_{c1} indicating the surface cracking, which is followed by a severe fluctuation at L_{c2} denoting the total delamination. The failure occurred under a critical load (L_{c1}) during the progressive mode with initial cracking, which is followed by the total delamination of the coated layer at the second critical load (L_{c2}).

Accordingly, Figure 5 shows the SEM micrographs from worn surfaces, which depict the higher critical distances of crack initiation and delamination for the BG-2GO sample. In another word, the BG-2GO sample sustained a higher normal load before failure.

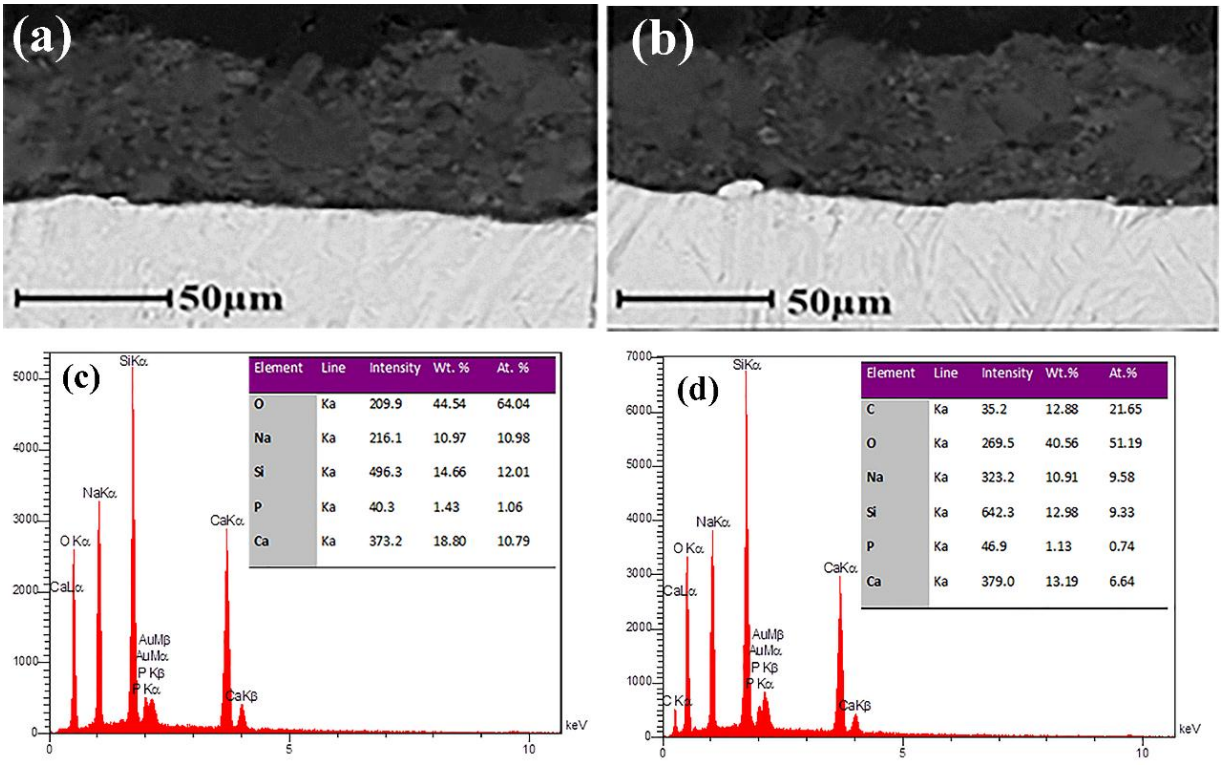

Figure 2. SEM micrographs and EDS spectra from cross-sectional views of (a,c) BG and (b,d) BG-2GO coatings

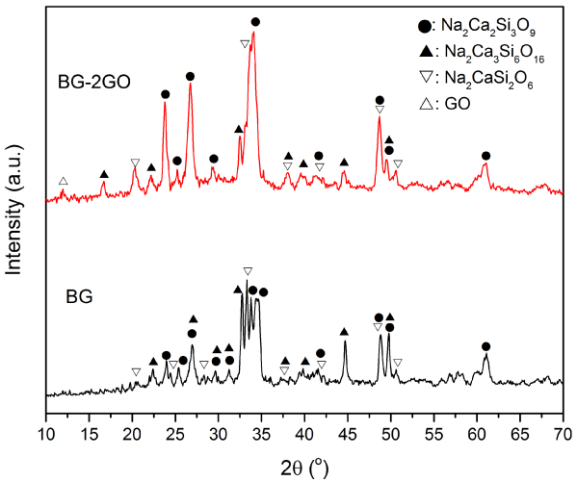

Figure 3. XRD patterns of BG and BG-2GO coated samples

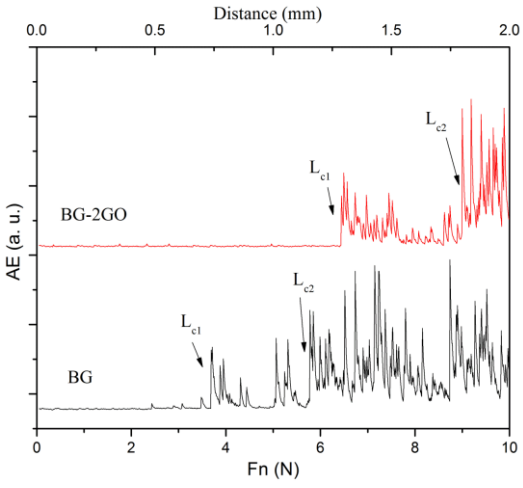

Figure 4. Acoustic emission (AE %) vs. scratching distance and progressive normal load for BG and BG-2GO samples

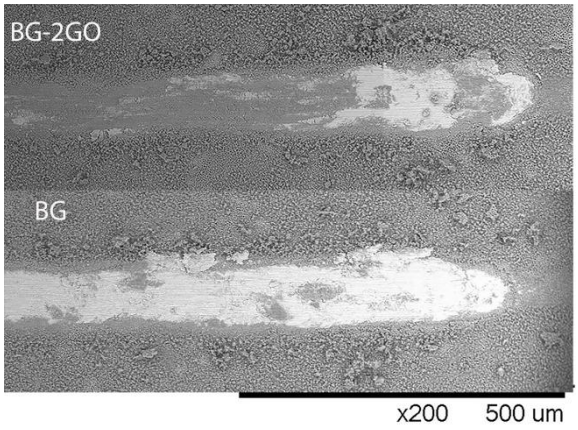

Figure 5. SEM micrographs of scratch grooves for BG and BG-2GO samples

Figure 6a and b summarize the critical loads and contact pressures of BG and BG-2GO samples. The highest critical contact pressures of P_{c1}=4.80GPa and P_{c2}=5.37GPa are estimated for the BG-2GO sample. This can be compared with the hardness of human bone, which varies between 0.5 and 0.75GPa [15]. It is evident from micro scratch analysis that GO can effectively inhibit crack initiation and propagation. It can be concluded that the addition of GO to the coating increases the density and hardness of the coating. Therefore, the critical pressure values obtained from the BG-2GO sample indicate an improvement in the mechanical properties of coated samples. The mechanism that resists cracking propagation by GO is frictional pullout, crack deflection, and crack bridging [16]. It is assumed that the grain bridging by GO sheets has a fundamental role in inhibiting crack propagation along the grain boundary. Furthermore, the high specific surface area of GO nano-sheet, makes it capable of forming an increased contact area with the matrix.

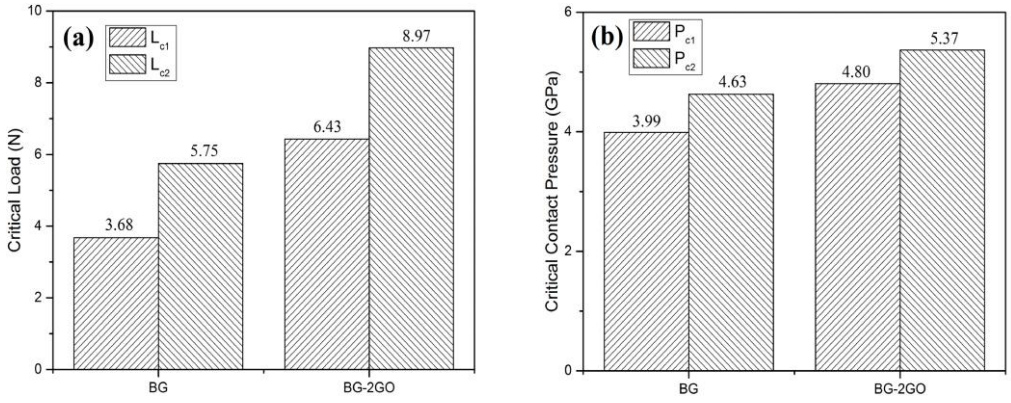

Figure 6. Critical contact (a) loads and (b) pressures of BG and BG-2GO samples

The implementation of a simple analytical linear elastic fracture mechanics model of the scratch test provides a means to determine the fracture toughness (K_c) from the forces measured during the test and to the geometry of the probe [17]:

$$K_c = \frac{F_T}{(2pA)^{1/2}} \quad (3)$$

Where F_T is the horizontal force, p is the perimeter, and A is the horizontal projected load bearing contact area. The determination of K_c requires knowing the variations of the indenter shape function (f) [17]:

$$f = 2p(d)A(d) \quad (4)$$

Where d is the penetration depth. For the studied indenter, $2pA.R^{-3}$ is determined in terms of $(d.R)^{-2}$ from the calibration curve [10].

According to Equation (3), the slope of linear variation of $F_T^2.R^{-3}$ against $2pA.R^{-3}$ in Figure 7 demonstrates the K_C^2 value. Moreover, the $F_T/[2pA]^{1/2}$ for penetration depths greater than half of the maximum depth ($d>d_{max}/2$) reaches a constant value indicating K_C in Figure 7.

Figure 8 illustrates the average fracture toughness of the coatings acquired by performing five scratches on each sample. The results depict that incorporation of GO into the coatings will increase K_C. Yazdanpanah et al. [18] showed that the fracture toughness of the BG-based nanocomposites increased with increasing the nanocrystalline forsterite content from 10 to 30wt% and

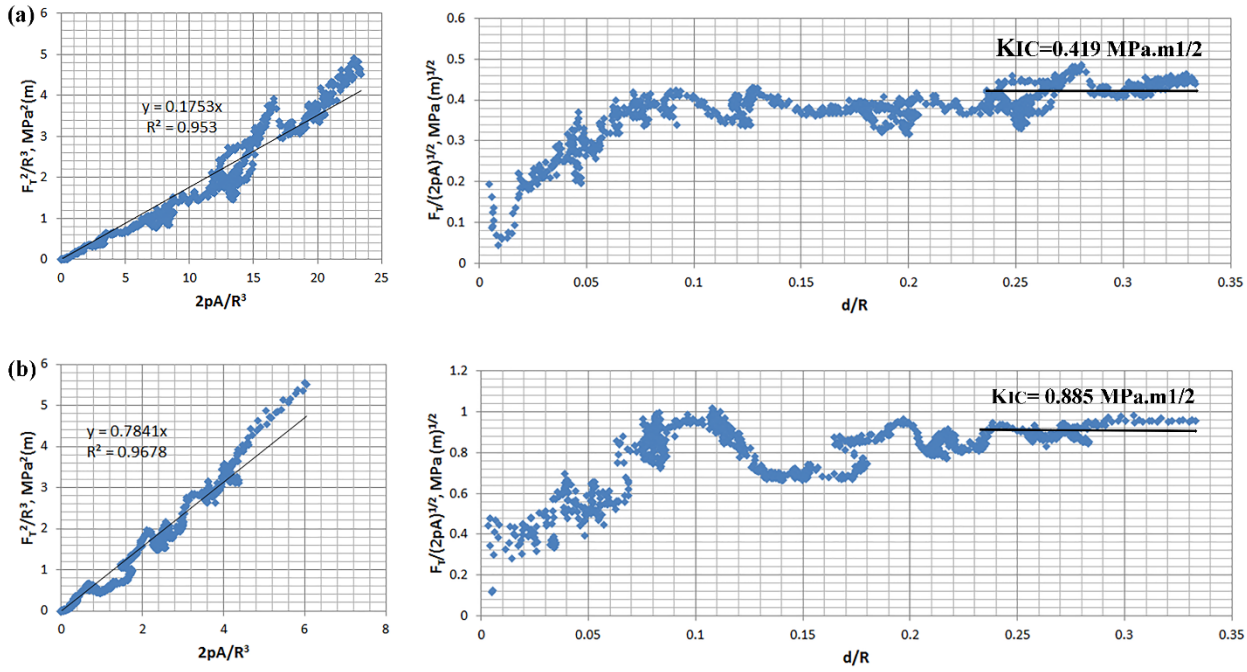

Figure 7. Variation of $F_T^2.R^{-3}$ against $2pA.R^{-3}$ and stress intensity factor (F_T /$[2pA]^{1/2}$) vs. d/R for (a) BG and (b) BG-2GO samples

the maximum fracture toughness of 0.22MPa.$m^{1/2}$ was achieved. Li et al. [19] considered the effect of the tensile residual stress on the crack propagation in an indentation test and reported the fracture toughness of 0.11MPa.$m^{1/2}$ for 45S5 bioglass. In the present study, the higher fracture toughness of 0.885MPa.$m^{1/2}$ was achieved for the BG-2GO sample, which is consistent with critical contact pressure results. The reduction in pores and microcracks can lead to the enhanced fracture toughness of the BG-2GO sample.

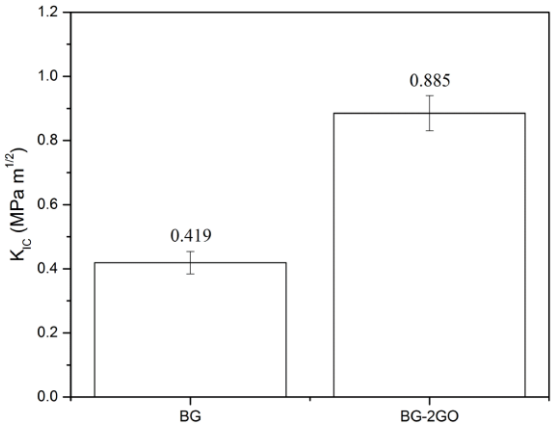

Figure 8. Fracture toughness estimated by micro scratch results for BG and BG-2GO samples

The increased fracture toughness of BG-GO coatings can be attributed to the toughening mechanism associated with grain bridging by GO nanosheets. This mechanism prevents crack propagation along the grain boundaries of the coating. Moreover, microstructural studies demonstrated that frictional pull-out, crack bridging, crack deflection, and crack tip shielding are responsible for the mechanical enhancement of graphene-based composites [16,20]. The highly-surface area GO nano-sheets with folding and twisted nanostructure morphology resulted in mechanical interlocking with BG particles. Also, the enhanced load transfer efficiency between the BG and GO causes an effective BG-based composite to increase the crack deflections by the effect of bridging of the GO nano-fillers [16,21].

4. CONCLUSION

The 45S5 bioglass-graphene oxide composite was deposited on Ti-6Al-4V alloy via electrophoretic deposition. The mechanical behavior of coatings was studied by using a micro scratch tester under a progressive load. The bonding strength of coatings was obtained by the calculation of critical contact pressures for crack initiation and delamination according to Hertz's theory. Based on the micro scratch analysis, the higher critical contact pressures of P_{c1}=4.80 and P_{c2}=5.37GPa,

were obtained for BG-GO composite coating. Moreover, the highest fracture toughness of K_{IC}=0.885MPa.$m^{1/2}$ was evaluated for BG-GO composite coating based on a linear elastic fracture mechanics model.

REFERENCES

1. Hosseini, S., Farnoush, H., "Characterization and in Vitro Bioactivity of Electrophoretically Deposited Mn-Modified Bioglass-Alginate Nanostructured Composite Coatings", ***Materials Research Express,*** Vol. 6, No. 2, (2018), 025404.
2. Farnoush, H., Mohandesi, J. A., Fatmehsari, D. H., "Effect of Particle Size on the Electrophoretic Deposition of Hydroxyapatite Coatings: A Kinetic Study Based on a Statistical Analysis", ***International Journal of Applied Ceramic Technology,*** Vol. 10, No. 1, (2013), 87-96.
3. Farnoush, H., Sadeghi, A., Abdi Bastami, A., Moztarzadeh, F., Aghazadeh Mohandesi, J., "An Innovative Fabrication of Nano-HA Coatings on Ti-CaP Nanocomposite Layer Using a Combination of Friction Stir Processing and Electrophoretic Deposition", ***Ceramics International,*** Vol. 39, No. 2, (2013), 1477-1483.
4. Farnoush, H., Abdi Bastami, A., Sadeghi, A., Aghazadeh Mohandesi, J., Moztarzadeh, F., "Tribological and Corrosion Behavior of Friction Stir Processed Ti-CaP Nanocomposites in Simulated Body Fluid Solution", ***Journal of Mechanical Behavior of Biomededical Materials,*** Vol. 20**,** **(**2013), 90-97.
5. Farnoush, H., Muhaffel, F., Cimenoglu, H., "Fabrication and Characterization of Nano-HA-45S5 Bioglass Composite Coatings on Calcium-Phosphate Containing Micro-Arc Oxidized CP-Ti Substrates", ***Applied Surface Science,*** Vol. 324, (2015), 765-774.
6. Boccaccini, A. R., Keim, S., Ma, R., Li, Y., Zhitomirsky, I., Boccaccini, A. R., Keim, S., Ma, R., Li, Y., Zhitomirsky, I., "Electrophoretic Deposition of Biomaterials Electrophoretic Deposition of Biomaterials", ***Journal of the Royal Society Interface,*** Vol. **7**, (2010), S581–S613.
7. Türk, M., Deliormanli, A. M., "Graphene-Containing PCL-Coated Porous 13-93B3 Bioactive Glass Scaffolds for Bone Regeneration", ***Materials Research Express,*** Vol. 5, No. 4, (2018), 45406.
8. Nguyen, B. H., Nguyen, V. H., "Promising Applications of Graphene and Graphene-Based Nanostructures", ***Advances in Natural Sciences: Nanoscience and Nanotechnology,*** Vol. 7, No. 2, (2016), 23002.
9. Yadav, N., Lochab, B., "A Comparative Study of Graphene Oxide: Hummers, Intermediate and Improved Method", ***FlatChem,*** Vol. 13, (2019), 40–49.
10. Farnoush, H., Aghazadeh Mohandesi, J., Çimenoğlu, H., "Micro-Scratch and Corrosion Behavior of Functionally Graded HA-TiO_2 Nanostructured Composite Coatings Fabricated by Electrophoretic Deposition", ***Journal of Mechanical Behavior of Biomededical Materials,*** Vol. 46, **(**2015), 31-40.
11. Sun, L., Fugetsu, B., "Mass Production of Graphene Oxide from Expanded Graphite", ***Materials Letters,*** Vol. 109, (2013), 207–210.
12. Dao, T. D., Jeong, H. M., "Graphene Prepared by Thermal Reduction–exfoliation of Graphite Oxide: Effect of Raw Graphite Particle Size on the Properties of Graphite Oxide and Graphene", ***Materials Research Bulletin,*** Vol. 70, (2015), 651–657.
13. Chen, J., Yao, B., Li, C., Shi, G., "An Improved Hummers Method for Eco-Friendly Synthesis of Graphene Oxide", ***Carbon,*** Vol. 64, (2013), 225–229.
14. Faure, J., Drevet, R., Lemelle, A., Ben Jaber, N., Tara, A., El Btaouri, H., Benhayoune, H., "A New Sol-Gel Synthesis of 45S5 Bioactive Glass Using an Organic Acid as Catalyst," ***Materials Science and Engineering C,*** Vol. 47, (2015), 407–412.
15. Farnoush, H., Rezaei, Z., "Effect of Suspension Stability on Bonding Strength and Electrochemical Behavior of Electrophoretically Deposited HA-YSZ Nanostructured Composite Coatings", ***Ceramics International,*** Vol. 43, (2016), 11885-11897.
16. Zhang, L., Liu, W., Yue, C., Zhang, T., Li, P., Xing, Z., Chen, Y., "A Tough Graphene Nanosheet/hydroxyapatite Composite with Improved in Vitro Biocompatibility", ***Carbon,*** Vol. 61, (2013), 105–115.
17. Akono, A.-T., Randall, N. X., and Ulm, F.-J., "Experimental Determination of the Fracture Toughness via Microscratch Tests: Application to Polymers, Ceramics, and Metals", ***Journal of Materials Research,*** Vol. 27, No 2, (2012), 485–493.
18. Yazdanpanah, A., Kamalian, R., Moztarzadeh, F., Mozafari, M., Ravarian, R., Tayebi, L., "Enhancement of Fracture Toughness in Bioactive Glass-Based Nanocomposites with Nanocrystalline Forsterite as Advanced Biomaterials for Bone Tissue Engineering Applications", ***Ceramics International***, Vol. 38, No 6, (2012), 5007–5014.
19. Li, D., Yang, F., Nychka, J., "Indentation-Induced Residual Stresses in 45S5 Bioglass and the Stress Effect on the Material Dissolution", ***Engineering Fracture Mechanics,*** Vol. 75, No 17, (2008), 4898–4908.
20. Gao, F., Xu, C., Hu, H., Wang, Q., Gao, Y., Chen, H., Guo, Q., Chen, D., Eder, D., "Biomimetic Synthesis and Characterization of Hydroxyapatite/graphene Oxide Hybrid Coating on Mg Alloy with Enhanced Corrosion Resistance", ***Materials Letters,*** Vol. 138, (2015), 25–28.
21. Li, H., Khor, K. A., Cheang, P., "Titanium Dioxide Reinforced Hydroxyapatite Coatings Deposited by High Velocity Oxy-Fuel (HVOF) Spray", ***Biomaterials,*** Vol. 23, No 1, (2002), 85–91.